Contents lists available at GrowingScience

Current Chemistry Letters

homepage: www.GrowingScience.com

Experimental and theoretical correlations in (*Z*)-C-aryl-N-methylnitrones

Karolina Kula[a*], Paulina Bierczak[a], Klaudia Miernik[a], Beata Synkiewicz-Musialska[a,b*] and Gajendra Kumar Gaurav[c,d]

[a]*Department of Organic Chemistry and Technology, Cracow University of Technology, Warszawska 24, 31-155 Cracow, Poland*
[b]*Institute of Microelectronics and Photonics, Łukasiewicz Research Network, Zabłocie 39, 30-701 Cracow, Poland*
[c]*Department of Chemical Engineering, Parul Institute of Technology, Parul University, Post Limda 391760 Waghodia, Gujarat, India*
[d]*Sustainable Process Integration Laboratory SPIL, Brno University of Technology, Technická 2896/2, 616-69, Brno, Czech Republic*

C H R O N I C L E

Article history:
Received February 28, 2024
Received in revised form
March 31, 2024
Accepted August 13, 2024
Available online
August 13, 2024

Keywords:
Nitrones
Hammett correlations
Taft correlations
Brown and Okamoto's correlations
Exner correlations
Inductive effect
Resonance effect
Reactivity descriptors
Global electronic properties

A B S T R A C T

Nitrones are an interesting group of organic compounds due to their spin-trapping properties. These chemical compounds are also useful building blocks via cycloaddition reactions. In this work, a comprehensive study about correlation of selected parameters come from quantum chemical and experimental studies, namely ^{1}H chemical shifts, IR absorption bands and UV-Vis maximum absorptions as well as reactivity descriptors such as global electrophilicity and nucleophilicity with substituent constants of *Hammett*, *Taft*, *Brown and Okamoto's* as well as *Exner* for *para* substituent analogues of *(Z)*-C-phenyl-N-methylnitrones have been study. Based on presented results it should be noted that tested models of substituent constants correlate in a satisfactory way with computational data. The opposite conclusion is observed for spectral data derived from analysis performed for synthesized nitrones. The obtained results constitute a useful element for future research on reaction mechanisms involving the tested nitrones.

1. Introduction

Nitrones, namely also imine N-oxides, are heteroorganic compounds having a characteristic iminoxy group in their structure (**Fig. 1**).[1] Compounds of this class are widespread in modern chemistry.[2,3] This is due to their unique properties, because nitrones are chemically similar in reactivity to carbonyl compounds such as ketones and aldehydes. Thanks to this, nitrones are useful in reactions with nucleophilic agents.[4]

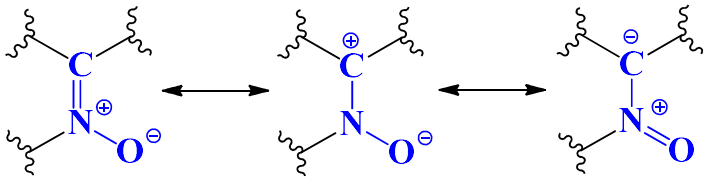

Fig. 1. Resonance structures of nitrones.

* Corresponding author
E-mail address karolina.kula@pk.edu.pl (K. Kula)

doi: 10.5267/j.ccl.2024.8.002

First of all, nitrones as nitrogen containing organic compounds[5,6] themselves have biological potential. The main use of these compounds consists in their application as spin-trapping agents to detect and identify transient radicals.[7] In a course of reaction between nitrone and radicals, the aminoxyl in a form of spin adducts are created (**Scheme 1**). Spin trapping is one of the very few analytical techniques that can identify the nature or structure of a radical intermediate. The EPR signal that is produced by the aminoxyl spin adduct provides a wealth of information due to their ability to not only quantify the number of radicals produced but also to identify radicals rather than just detect them, which is one unique feature of spin trapping over the use of other techniques. A unique feature of the spin-trapping technique is its ability to discern various radicals formed from each other based on their spectral profiles of their spin adduct. Therefore, with spin trapping, one could differentiate O-centered radicals such as $O^{2\bullet-}$, $HO^{\bullet}$, and $RO^{\bullet}$ as well as C, N, and S radicals.[8,9]

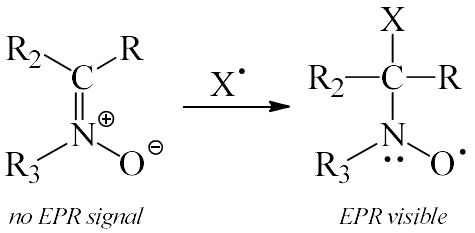

Scheme 1. Formation of aminoxyl spin adduct from nitrones.

The presented application of nitrones is commonly used in trapping free radicals generated inside the cells and tissues. The first mentions about this topic come from the mid-1980s. In 1986 *Novelli et al.* reported that administration of *(Z)*-C-phenyl-N-*tert*-butyl nitrone, (PBN) (**Fig. 2**), confers protection on rats from lethal whole-body trauma or circulatory shock.[10] In turn, in 2001 *Zhao et al.* tested another PBN derivative, which was *(Z)*-2,4-disulfophenyl-N-tert-butylnitrone, referred to as NXY-059 (**Fig. 2**). This nitrone was the first example of spin-trapping agent to reach Phase III clinical trials in the USA for the treatment of acute ischemic stroke.[11] Currently, these compounds are used in medicine against several ROS-related disorders, such as brain injury,[12] renal injury,[13] visual loss,[14] as well as neuronal damage.[15] In the next years, the anticancer role of PBN and its derivatives against various types of cancer was also studied. These nitrones are reported to inhibit tumor growth and progression in hepatocellular carcinoma, brain cancer and colon cancer models.[16,17] Next to linear nitrones such as PBN and also NXY-059, in the literature there are several examples of cyclic nitrones used as trapping free radicals. In 2009 *Zuo et al.* reported about the cardio-protective functions of the cyclic nitrone, 5,5-dimethyl-1-pyrroline N-oxide (DMPO) (**Fig. 2**), against I/R injury.[18]

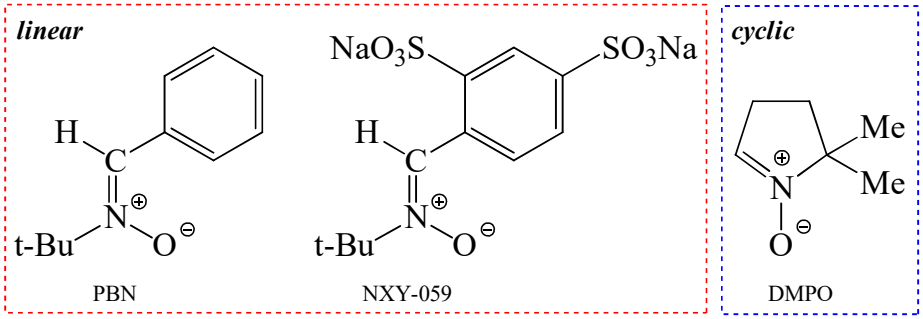

Fig. 2. Common cyclic and linear nitrones used as spin-trapping agents.

Nitrones have also found application in the fields of photodynamic therapy,[19] fuel cell research,[20] nanotechnology,[21] as well as catalysis.[22] However, except for their biological importance, these chemical compounds are widely used as important building blocks in the synthesis of heterocycles. In particular, nitrones are used as three atoms components[23,24] *via* reactions [3+2] cycloaddition (32CA).[25,26] As a result of these reactions, it is possible to obtain isoxazolines as well as isoxazolines (**Scheme 2**).[27-29]

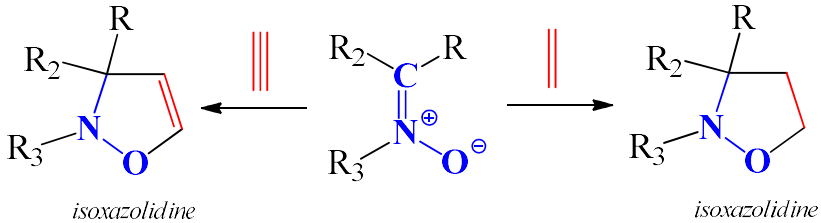

Scheme 2. Explanatory scheme of application of nitrone *via* 32CA with acetylene and acetylene systems.

Therefore, taking into account both the significant biological potential as well as the usefulness in the synthesis of heterocycles, it was decided to carry out the study about the substituent effect for the selected series of *para* substituent analogues of *(Z)*-C-phenyl-N-methylnitrones. This type of research is particularly desirable for scientists studying reaction mechanisms. For this purpose the substituent constants of *Hammett*[30] (representing the total of inductive and resonance effects), *Taft*[31] (representing the total the inductive and resonance effects without strong resonance interactions between substituents and the reaction centre), *Brown and Okamoto's*[32] (representing the total the inductive and resonance effects with strong resonance interactions between substituents and the reaction centre) as well as *Exner*[33] (representing separate the inductive or resonance effects) had been applied. Present research was explored on two independent approaches, namely in an experimental way as well as based on quantum chemical calculations.

2. Results and Discussion

2.1. Selection of nitrones used in the presented study

The choice of nitrones tested in this article was dictated by two main criteria. One of them is the availability of reagents necessary to carry out the synthesis. The second one was the fact of having biological activity through nitrones. Therefore, the basic physicochemical parameters for selected nitrones were simulated by SwissADME.[34] The obtained data were evaluated using a drug-likeness model via rules of *Lipinski et al.*[35] Additionally, in order to emphasize the authenticity of the analysis performed, the potential use of selected nitrones was tested using the PASS program.[36]

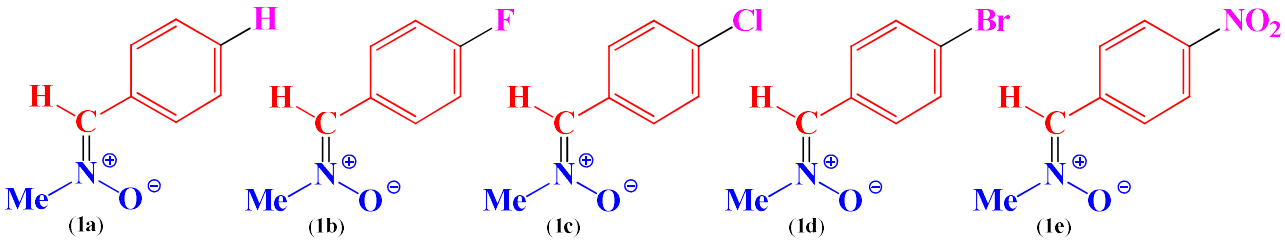

Fig. 3. Structures of tested *para* substituent analogues of *(Z)*-C-aryl-N-methylnitrones (**1a-e**).

Taking into account the above-mentioned elements, the homologous series of *para* substituent analogues of *(Z)*-C-phenyl -N-methylnitrones **1a-e** as the tested nitrones were analysed (**Fig. 3**). These compounds **1a-e** have been evaluated according to *Lipinski et al.*[35] rules. Based on information collected in **Table 1** it can be concluded that all selected nitrones **1a-e** are characterized by appropriate lipophilicity, quantity of H-bond acceptors and donors as well as molecular weight.

Table 1. The selected physicochemical parameters of tested *para* substituent analogues of *(Z)*-C-phenyl-N-methylnitrone (**1a-e**) together with evaluation according to *Lipinski et al.*[35] rules.

	Nitrone					***Lipinski et al.*[35] range**	
	1a	**1b**	**1c**	**1d**	**1e**		
Molecular weight [Da]	135	153	169.5	214	180	**≤ 500 Da**	✓
#H-bond acceptors	1	2	1	1	3	**≤ 10**	✓
#H-bond donors	0	1	0	0	0	**≤ 5**	✓
Lipophilicity Log $P_{o/w}$	1.66	2.09	2.25	2.40	0.49	**≤ 4.15**	✓

In order to explain a biological potential of selected *para* substituent analogues of *(Z)*-C-phenyl-N-methylnitrone **1a-e** the PASS[36] analysis has been performed. **Table 2** contains the most probable direction for biological implementation. According to PASS analysis it should be noted that for all selected nitrones **1a-e** can be applied as cerebral anti-ischemic agents as well as in a role of interleukin antagonist.

Table 2. Prediction of the main biological activities of tested *para* substituent analogues of *(Z)*-C-phenyl-N-methylnitrone (**1a-e**) using PASS.[36] The results are expressed as molecule's probability to be active (Pa) or inactive (Pi).

	Activity	**Pa**	**Pi**
1a	Antiischemic, cerebral	0.950	0.004
	Interleukin antagonist	0.909	0.003
1b	Antiischemic, cerebral	0.926	0.005
	Interleukin antagonist	0.900	0.003
1c	Antiischemic, cerebral	0.930	0.005
	Interleukin antagonist	0.886	0.003
1d	Interleukin antagonist	0.883	0.003
	Antiischemic, cerebral	0.878	0.007
1e	Antiischemic, cerebral	0.902	0.005
	Interleukin antagonist	0.879	0.003

Therefore, both analysis of the physicochemical parameters as well as the prediction of the main biological activities show that the chosen nitrones (**1a-e**) are valuable candidates for testing due to their potential properties.

2.2. Synthesis and spectral characteristic of tested nitrones

Many methods for the synthesis of nitrones are available. To the most popular laboratory protocols include imine oxidation,[37,38] alkylation and arylation of oximes,[39,40] as well as condensation reactions of N-substituted hydroxylamines with aldehydes or ketones.[41-43] In the presented work, the last method has been applied. For this purpose, in a role of substrates *para* substituent analogues of benzaldehyde (**2a-e**) and N-methylhydroxylamine hydrochloride (**3**) were used (**Scheme 3**). The choice of the synthesis method for the tested nitrones (**1a-e**) was dictated by several aspects: (I) common and simple protocol; (II) availability of necessary reagents; (III) high yields of the final products.

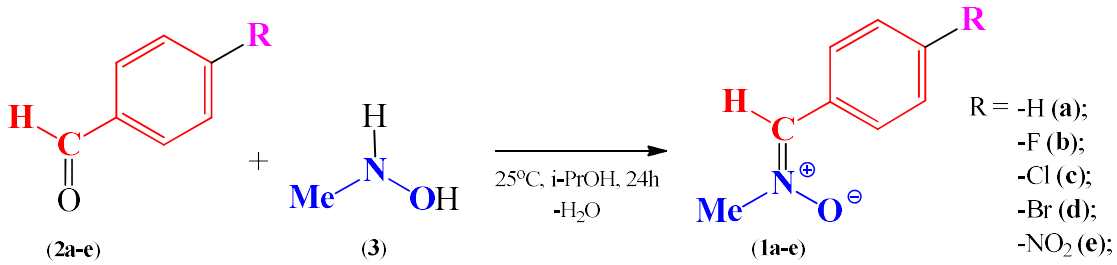

Scheme 3. Synthesis of the tested nitrones (1a-e) via condensation reaction between *para* substituent analogues of benzaldehyde (**2a-e**) N-methylhydroxylamine hydrochloride (**3**).

First, the simplest *(Z)*-C-phenyl-N-methylnitrone (**1a**) has been synthesized. Searching for most convenient conditions for carrying out this synthesis, several attempts of reaction have been made, changing the molar ratio of the reactants, the used solvent, the reaction temperature as well as access to light (**Table 3**). On this basis, the most favourable conditions for synthesis have been determined as the room temperature in the dark, and the use of isopropanol as the solvent. The optimal moral ratio of reactants is the excess of hydroxylamine relative to aldehyde (**Table 3**).

Table 3. Optimization of reaction conditions for the sysnthesis of *(Z)*-C-phenyl-N-methylnitrone (**1a**).

Molar ratio 2a : 3	Solvent	Temperature	Access to light	Reaction yield
1 : 1	Toluene	Reflux	Yes	-
1.2 : 1	Toluene	Reflux	Yes	-
1 : 1.2	Toluene	Reflux	Yes	-
1 : 1	Toluene	Reflux	No	54%
1.2 : 1	Toluene	Reflux	No	44%
1 : 1.2	Toluene	Reflux	No	56%
1 : 1	Toluene	Room temp.	No	75%
1 : 1.2	Toluene	Room temp.	No	83%
1 : 1	Isopropanol	Room temp.	No	88%
1 : 1.2	**Isopropanol**	**Room temp.**	**No**	**92%**

In order to generate N-methyl-hydroxylamine (**3**) from its hydrochloride form, sodium bicarbonate was used. In turn, in order to absorb water formed during the reaction, the sodium sulfate was applied. The reaction progress was monitored via HPLC Under presented conditions and using the mentioned reagents, the conversion of the substrates lasted 24 hours. First, the solvent was distilled from the obtained post-reaction mass using a vacuum evaporator under reduced pressure. In order to separate the potential nitrone **1a** from the remains of unreacted substrates and other inorganic compounds, the extraction of dichloromethane has been applied. Finally, the reaction product was purified by crystallization from methyl alcohol. The hypothetical *(Z)*-C-phenyl-N-methylnitrone (**1a**) was obtained as white, crystalline solid. The syntheses of the remaining nitrones **1b-e** were carried out according to the presented protocol.

The constitution of *para* substituent analogues of *(Z)*-C-phenyl-N-methylnitrones **1a-e** have been confirmed based on spectroscopic and physicochemical analysis. It should be underlined that obtained compounds are not novel connections and they have been characterized in the past. So, first of all, melting points for all products were determined. Values for the obtained connections are compatible with literature melting points for nitrones **1a-e**. Based on this information, it may be presumed that synthesized compounds are expected to be nitrones **1a-e**. The similar situation is observed in a case of UV-Vis analysis. In particular, measured absorption maxima for obtained connections are identical to the case of expected nitrones **1a-e**.

The analyses that fully explain the structure of the obtained compounds are ^{1}H NMR and IR. The significant for these considerations were the identification of (I) singlet in ^{1}H NMR spectra, relating to the methyl group, as well as (II) signals relating to the iminoxy moiety in IR spectra. The most important results of performed analysis are collected in **Table 4**.

Table 4. Selected physicochemical and spectral data for tested *para* substituent analogues of *(Z)*-C-phenyl-N-methylnitrones **1a-e**.

	R_t [min]	t_t [°C]	UV-Vis [nm] λ_{max}	^{1}H NMR [ppm] δ C<u>H</u>$_3$	IR [cm^{-1}] υ >C=$^+$N<	IR [cm^{-1}] υ >N$^+$→O$^-$
1a	3.13	80	288	3.78	1594	1163
1b	3.42	109	287	3.79	1596	1232
1c	4.50	132	305	3.80	1591	1165
1d	5.00	139	297	3.79	1581	1161
1e	3.58	212	293	3.78	1597	1333

2.3. Correlation of substituent constants with theoretical parameters

First, it was decided to determine basic reactivity descriptors for the tested *para* substituent analogues of *(Z)*-C-phenyl-N-methylnitrones **1a-e**. For this purpose, the well-established approach of Conceptual Density Functional Theory (CDFT) was used.[44] The CDFT is a very important tool in understanding the reactivity of molecules in polar processes.[45] The theory is to connect well established chemical concepts, like electronic chemical potential μ and chemical hardness η with the electronic structure of a molecule. Based on those, the indication of global electronic properties of substrates, such as global electrophilicity ω and global nucleophilicity N for molecules, can be established. As an effect, it is possible to assign addends a role of either an electrophile or a nucleophile in studied reactions.[46,47] Furthermore, with application of Parr functions, not only global, but also local electronic properties of a molecule can be estimated, thus allowing to predict reactivity of molecules in the studied reactions, based only on substrates structures.[48] Thus, the global reactivity indices for the *para* substituent analogues of *(Z)*-C-phenyl-N-methylnitrones **1a-e** are presented in **Table 5**.

Table 5. HOMO and LUMO energies as well as global reactivity indices given in electronvolts [eV] for tested *para* substituent analogues of *(Z)*-C-phenyl-N-methylnitrones **1a-e**, according to B3LYP/6-31G(d) in gas phase.

	HOMO energy [eV]	LUMO energy [eV]	Chemical potential μ [eV]	Chemical hardness η [eV]	Global electrophilicity index ω [eV]	Global nucleophilicity index N [eV]
1a	-5.50	-1.27	-3.39	4.24	1.35	3.62
1b	-5.55	-1.31	-3.43	4.24	1.39	3.57
1c	-5.68	-1.53	-3.61	4.15	1.57	3.44
1d	-5.67	-1.54	-3.61	4.13	1.57	3.45
1e	-6.23	-2.64	-4.43	3.59	2.74	2.89

Based on the obtained computational results, it is possible to determine the nature of the tested nitrones **1a-e**. The simplest *(Z)*-C-phenyl-N-methylnitrone (**1a**) the calculated value of global electrophilicity for this nitrone is 1.35 eV, and the calculated value of global nucleophilicity is 3.62 eV (**Table 5**). This means that the nitrone **1a** can be classified as both a moderate electrophile and a strong nucleophile. Replacing the hydrogen atom in the para position of the phenyl ring in nitrones **1b-d** on the halogen atom does not significantly change the nature of the molecules. In particular, the nucleophilicity index of nitrones **1b-d** is slightly reduces, to 3.57 (**1b**), 3.44 (**1c**) and 3.45 (**1d**) eV, as well as the electrophilicity index of nitrones **1b-d** slightly increases, to 1.39 (**1b**), 1,57 (**1c**) and 1.57 (**1d**) eV (**Table 5**). As a consequence, all mentioned *(Z)*-C-aryl-N-methylnitrones **1b-d** can be considered as moderate electrophiles and also strong nucleophiles. Another situation is observed for introducing a strong electron-withdrawing substituent which is the nitro group. Both global electrophilicity and nucleophilicity indexes have changed considerably. In particular, the nucleophilicity index of nitrone **1e** is drastically reduces, to 2.89 eV, as well as the electrophilicity index of nitrones **1e** drastically increases, to 2.74 eV (**Table 5**). In a consequence, the *(Z)*-C-(4-nitrophenyl)-N-methylnitrone **1e** can be considered as a strong electrophile and also a moderate nucleophile.

In the next part of presented research, it was decided to compare the obtained values of global electrophilicity and nucleophilicity (**Table 5**) with substituent constants according to *Hammett* (σ_p),[30] *Taft* (σ_p^0),[31] *Brown and Okamoto's* (σ_p^+)[32] as well as *Exner* (σ_I and σ_R)[33] for *para* substituent analogues of *(Z)*-C-phenyl-N-methylnitrones **1a-e**. The correlations include the selected quantum-chemical calculation results collected in **Table 6**.

Table 6. Correlation between selected substituent constants and global electrophilicity and nucleophilicity for tested *para* substituent analogues of *(Z)*-C-phenyl-N-methylnitrones **1a-e**.

Dependency type	Linear regression	R^2
Hammett constants σ_p vs. global electrophilicity index ω	$\sigma_p = 1.85 \cdot \omega + 1.24$	0.9738
Hammett constants σ_p vs. global nucleophilicity index N	$\sigma_p = -0.95 \cdot N + 3.64$	0.9947
Taft constants σ_p^0 vs. global electrophilicity index ω	$\sigma_p^0 = 1.83 \cdot \omega + 1.17$	0.9549
Taft constants σ_p^0 vs. global nucleophilicity index N	$\sigma_p^0 = -0.94 \cdot N + 3.68$	0.9793
Brown and Okamoto's constants σ_p^+ vs. global electrophilicity index ω	$\sigma_p^+ = 1.67 \cdot \omega + 1.40$	0.9843
Brown and Okamoto's constants σ_p^+ vs. global nucleophilicity index N	$\sigma_p^+ = -0.84 \cdot N + 3.56$	0.9794
Exner induction constants σ_I vs. global electrophilicity index ω	$\sigma_I = 1.30 \cdot \omega + 1.13$	0.3606
Exner induction constants σ_I vs. global nucleophilicity index N	$\sigma_I = -0.72 \cdot N + 3.72$	0.4255
Exner resonance constants σ_R vs. global electrophilicity index ω	$\sigma_R = 1.17 \cdot \omega + 2.03$	0.2680
Exner resonance constants σ_R vs. global nucleophilicity index N	$\sigma_R = -0.54 \cdot N + 3.26$	0.2187

In the case of correlation studies for the substituent effect in organic compounds containing substituents directly connected with the aromatic ring, *Jaffe* described that a determination coefficient R^2 above 0.99 indicates an excellent fit and a satisfactory and fair fits range from 0.99 to 0.90. In turn, determination coefficient R^2 below 0.90 are considered as not being adequately.[49]

Based on the data in **Table 6**, as well as the ranges identified by *Jeff*[49] it should be concluded that both of *Hammett*, *Taft* as well as *Brown and Okamoto's* substituent constants correlate in more than satisfactory way with global electronic properties of tested *para* substituent analogues of *(Z)*-C-phenyl-N-methylnitrones **1a-e**. In particular, in a case of correlation of *Hammett* substituent constants for global electrophilicity indexes the determination coefficient R^2 is satisfactory (0.9738) and for global nucleophilicity indexes the determination coefficient R^2 is excellent (0.9947) (**Table 6**). Similar results were received for correlation of *Brown and Okamoto's* substituent constants with global electrophilicity indexes (0.9843; satisfactory kind of fit) and with global nucleophilicity indexes (0.9794; satisfactory kind of fit) (**Table 6**). Slightly worse but still acceptable results were obtained for correlation of *Taft* substituent constants with global electrophilicity indexes (0.9549; satisfactory kind of fit) and with global nucleophilicity indexes (0.9793; satisfactory kind of fit) (**Table 6**).

A completely different situation is observed in the case of correlations of global electronic properties with both *Exner* constants. In particular, all of the mentioned correlations have values less than 0.5 which means that they are considered as not being adequate according to *Jeff*[49] recommendation. However, taking into account the separated inductive and resonance effects for the series of tested *para* substituent analogues of *(Z)*-C-phenyl-N-methylnitrones **1a-e**, higher values of the determination coefficient R^2 are obtained in the case of correlation of global reactivity descriptors with *Exner* constants representing the inductive effect. For correlation of *Exner* substituent constants for global electrophilicity indexes the determination coefficient R^2 for inductive effect is 0.3606 and for resonance effect is 0.2680. In turn, for correlation of *Exner* substituent constants for global nucleophilicity indexes the determination coefficient R^2 for inductive effect is 0.2680 and for resonance effect is 0.2187. and for global nucleophilicity index the determination coefficient R^2 is excellent (0.9947) (**Table 6**).

Taking into account the correlations of the global reactivity descriptors with all tested substituent constants, it should be concluded that the best results are obtained when using substituent constants representing the sum of inductive and resonance effects. Global electrophilicity values have the best correlation with *Brown and Okamoto's* substituent constants. In turn, global nucleophilicity values have the best correlation with *Hammett* substituent constants. For the series of tested *para* substituent analogues of *(Z)*-C-phenyl-N-methylnitrones **1a-e**, the dominant effect caused by the substituent is inductive effect arising from differences in electronegativity between bonded atoms, which leads to a polarisation of the bond.[50,51]

2.4. Correlation of substituent constants with experimental parameters

The obtained compounds were tested to confirm their constitution. The results of these analyzes were compared with literature data.[52,53] In the next part of the presented study, it was decided to compare selected characteristic spectral data with the tested substituent constants. For this purpose, UV-Vis, IR as well as NMR analysis data were used (**Table 4**). The correlations include the selected experimental results collected in **Table 7**.

Table 7. Correlation between selected substituent constants and key spectroscopic parameters for tested *para* substituent analogues of *(Z)*-C-phenyl-N-methylnitrones **1a-e**.

Dependency type	Linear regression	R^2
Hammett constants σ_p vs. λ_{max} of UV-Vis	$\sigma_p = 5.25 \cdot \lambda + 292.63$	0.0482
Hammett constants σ_p vs. proton shift δ C$\underline{H}_3$ of ^{1}H NMR	$\sigma_p = -0.01 \cdot \delta + 3.79$	0.0803
Hammett constants σp vs. signal υ >C=$^+$N< of IR	$\sigma_p = 4.29 \cdot \upsilon + 1590.7$	0.0417
Hammett constants σ_p vs. signal υ >N$^+$→O$^-$ of IR	$\sigma_p = 197.44 \cdot \upsilon + 1159.5$	0.6607
Taft constants σ_p^0 vs. λ_{max} of UV-Vis	$\sigma_p^0 = 2.8843 \cdot \lambda + 293.43$	0.0182
Taft constants σ_p^0 vs. proton shift δ C$\underline{H}_3$ of ^{1}H NMR	$\sigma_p^0 = -0.0103 \cdot \delta + 3.79$	0.1774
Taft constants σ_p^0 vs. signal υ >C=$^+$N< of IR	$\sigma_p^0 = 4.47 \cdot \upsilon + 1590.9$	0.0564
Taft constants σ_p^0 vs. signal υ >N$^+$→O$^-$ of IR	$\sigma_p^0 = 175.06 \cdot \upsilon + 1176.5$	0.6496
Brown and Okamoto's constants σ_p^+ vs. λ_{max} of UV-Vis	$\sigma_p^+ = 4.5823 \cdot \lambda + 292.61$	0.0369
Brown and Okamoto's constants σ_p^+ vs. proton shift δ C$\underline{H}_3$ of ^{1}H NMR	$\sigma_p^+ = -0.0065 \cdot \delta + 3.79$	0.0569
Brown and Okamoto's constants σ_p^+ vs. signal υ >C=$^+$N< of IR	$\sigma_p^+ = 5.15 \cdot \upsilon + 1590.2$	0.0603
Brown and Okamoto's constants σ_p^+ vs. signal υ >N$^+$→O$^-$ of IR	$\sigma_p^+ = 206.72 \cdot \upsilon + 1148$	0.7294
Exner induction constants σ_I vs. λ_{max} of UV-Vis	$\sigma_I = 8.7949 \cdot \lambda + 290.01$	0.0914
Exner induction constants σ_I vs. proton shift δ C$\underline{H}_3$ of ^{1}H NMR	$\sigma_I = 0.0093 \cdot \delta + 3.7838$	0.0879
Exner induction constants σ_I vs. signal υ >C=$^+$N< of IR	$\sigma_I = 0.65 \cdot \upsilon + 1591.5$	0.0007
Exner induction constants σ_I vs. signal υ >N$^+$→O$^-$ of IR	$\sigma_I = 173.62 \cdot \upsilon + 1132$	0.3836
Exner resonance constants σ_R vs. λ_{max} of UV-Vis	$\sigma_R = -3.2632 \cdot \lambda + 293.16$	0.0128
Exner resonance constants σ_R vs. proton shift δ C$\underline{H}_3$ of ^{1}H NMR	$\sigma_R = -0.0237 \cdot \delta + 3.7819$	0.5237
Exner resonance constants σ_R vs. signal υ >C=$^+$N< of IR	$\sigma_R = 5.69 \cdot \upsilon + 1593.3$	0.0506
Exner resonance constants σ_R vs. signal υ >N$^+$→O$^-$ of IR	$\sigma_R = 80.283 \cdot \upsilon + 1231.5$	0.0755

Based on the data in **Table 7**, as well as the ranges identified by *Jeff*[49] it should be concluded that all tested substituent constants do not show satisfactory correlation with selected spectroscopic parameters. In particular, the determination coefficient R^2 of correlation of *Hammett*, *Taft* as well as *Brown and Okamoto's* substituent constants with λ_{max} of UV-Vis, proton shift δ C<u>H</u>$_3$ of ^{1}H NMR and signal υ >C=$^+$N< of IR of tested nitrones **1a-e** do not even exceed 0.2000 (**Table 7**). One promoting dependency type is correlation for mentioned *Hammett*, *Taft* as well as *Brown and Okamoto's* substituent constants with signal υ >N$^+$→O$^-$ of IR. Nevertheless, the determination coefficient R^2 for these correlations still fluctuates in the range of ca. 0.65-0.73 (**Table 7**). Therefore, even these values are not sufficient according to the ranges defined by *Jeff*.[49] Based on the correlation between *Exner* substituent constants and selected spectroscopic parameters, it cannot be clearly stated which of the two effects, namely induction or resonance, is stronger for tested *para* substituent analogues of *(Z)*-C-phenyl-N-methylnitrones **1a-e**. In particular, the highest determination coefficient R^2 occurs for dependency of *Exner* resonance constants with proton shift δ C<u>H</u>$_3$ of ^{1}H NMR (0.5237) and the rest of determination coefficient R^2 do not even exceed 0.1000 (**Table 7**). Additionally, a determination coefficient R^2 coefficient occurs alternately. This means that in the case of *Exner* correlation with λ_{max} of UV-Vis the inductive effect prevails, while for proton shift δ C<u>H</u>$_3$ of ^{1}H NMR the resonance effect definitely prevails. In turn, for IR signals it is either inductive (signal υ >C=$^+$N<) or resonant (signal υ >N$^+$→O$^-$), depending on the considered band (**Table 7**).

3. Conclusions

The summary of the presented correlation research for tested *para* substituent analogues of *(Z)*-C-phenyl-N-methylnitrones **1a-e**, it should be concluded that computational parameters in a form of the global reactivity descriptors correlate in satisfactory way with all tested substituent constants. In particular, the best results are obtained when using substituent constants representing the sum of inductive and resonance effects. Global electrophilicity values have the best correlation with *Brown and Okamoto's* substituent constants. In turn, global nucleophilicity values have the best correlation with *Hammett* substituent constants. In turn, the dominant effect caused by the substituent is an inductive effect arising from differences in electronegativity between bonded atoms, which leads to a polarisation of the bond. In turn, in an experimental data it should be mentioned all tested substituent constants do not show satisfactory correlation with selected spectroscopic parameters. One promoting dependency type is correlation for mentioned *Hammett*, *Taft* as well as *Brown and Okamoto's* substituent constants with signal υ >N$^+$"O$^-$ of IR. Nevertheless, the determination coefficient R^2 for these correlations still fluctuates in the range of ca. 0.65-0.73, so even these values are not sufficient. What is more, it cannot be clearly stated which of the two effects, namely induction or resonance, is stronger for these correlations. The consistency in the obtained results is not observable.

4. Experimental

4.1. Materials and Methods

Commercially available (Sigma–Aldrich, Szelągowska 30, 61-626 Poznań, Poland) reagents and solvents were used. All reagents were tested with high pressure liquid chromatography before use.

4.2. Analytical Techniques

For reaction progress testing, high pressure liquid chromatography (HPLC) was performed a KNAUER apparatus equipped with a UV-Vis detector with application of the standard procedure.[54-56] LiChrospher RP-18 10 μm column (4 × 250 mm) was applied and methanol-water MeOH:H_2O (60:40 v/v) was used as eluent at a flow rate of 1.5 cm^3/min. Melting points were determined with the Boetius PHMK 05 apparatus and were not corrected. FT-IR spectra were derived from the FTS Nicolet IS 10 spectrophotometer with Attenuated Total Reflectance (ATR). ^{1}H NMR (60 MHz) spectra were recorded with a NANALYSIS 60e spectrometer. All spectra were obtained in the deuterated chloroform $CDCl_3$ (visible at 7.27 ppm for ^{1}H NMR) solutions and the chemical shifts (δ) are expressed in ppm. TMS was used as an internal standard. UV-Vis spectra were determined in methanolic solutions for the 190-500 nm range with a spectrometer UV-5100 BIOSENS. The maximum of absorption was detected below 1 AU of absorbance and adheres to Beer-Lambert Law.

*4.3. General synthesis procedure of (Z)-C-aryl-N-methylnitrones (**1a-e**)*

In an Erlenmeyer flask, equipped with a magnetic stirrer, 4 mmol of appropriate substituent analogue of benzaldehyde (**2a-e**), 5 mmol of N-methylhydroxylamine hydrochloride (**3**), 5 mmol of sodium bicarbonate, 5 mmol of anhydrous sodium sulfate and also 10 mL of anhydrous isopropyl alcohol. The mixture was stirred for 24 h without exposure to light. After this time, the solvent was evaporated. From the obtained precipitate, which was a mixture of organic and inorganic residue, I isolated the product by extraction from dichloromethane. The final nitrones (**1a-e**) were purified by crystallization from methanol.

4.4. Physical and Spectral Data

- *(Z)*-C-phenyl-N-methylnitrone (**1a**): white crystal solid; m.p. 80 °C; R_t (MeOH:H_2O 60:40 v/v): 3.13 min; UV-Vis (CH_3OH): λ_{max} [nm] 288; FT-IR (ATR): υ [cm^{-1}] 1594 (>C=$^+$N< nitrone moiety, strong), 1163 (>N$^+$→O$^-$ nitrone moiety, strong); ^{1}H NMR (60 MHz, $CDCl_3$): δ [ppm] 3.78 (s, 3H, -CH_3).

- *(Z)*-C-(4-fluorophenyl)-N-methylnitrone (**1b**): white crystal solid; m.p. 109 °C; R_t (MeOH:H_2O 60:40 v/v): 3.42 min; UV-Vis (CH_3OH): λ_{max} [nm] 287; FT-IR (ATR): υ [cm^{-1}] 1596 (>C=$^+$N< nitrone moiety, strong), 1232 (>N^+→O^- nitrone moiety, strong); ^{1}H NMR (60 MHz, $CDCl_3$): δ [ppm] 3.79 (s, 3H, -CH_3).
- *(Z)*-C(4-chlorophenyl)-N-methylnitrone (**1c**): white crystal solid; m.p. 132 °C; R_t (MeOH:H_2O 60:40 v/v): 4.50 min; UV-Vis (CH_3OH): λ_{max} [nm] 305; FT-IR (ATR): υ [cm^{-1}] 1591 (>C=$^+$N< nitrone moiety, strong), 1165 (>N^+→O^- nitrone moiety, strong); ^{1}H NMR (60 MHz, $CDCl_3$): δ [ppm] 3.80 (s, 3H, -CH_3).
- *(Z)*-C(4-bromophenyl)-N-methylnitrone (**1d**): white crystal solid; m.p. 139 °C; R_t (MeOH:H_2O 60:40 v/v): 5.00 min; UV-Vis (CH_3OH): λ_{max} [nm] 297; FT-IR (ATR): υ [cm^{-1}] 1581 (>C=$^+$N< nitrone moiety, strong), 1161 (>N^+→O^- nitrone moiety, strong); ^{1}H NMR (60 MHz, $CDCl_3$): δ [ppm] 3.79 (s, 3H, -CH_3).
- *(Z)*-C(4-nitrophenyl)-N-methylnitrone (**1e**): yellow crystal solid; m.p. 212 °C; R_t (MeOH:H_2O 60:40 v/v): 3.58 min; UV-Vis (CH_3OH): λ_{max} [nm] 293; FT-IR (ATR): υ [cm^{-1}] 1597 (>C=$^+$N< nitrone moiety, strong), 1333 (>N^+→O^- nitrone moiety, strong); ^{1}H NMR (60 MHz, $CDCl_3$): δ [ppm] 3.78 (s, 3H, -CH_3).

4.5. Computational Details

All computations were performed using the Gaussian 16 package[57] in the Ares computer cluster of the CYFRONET regional computer centre in Cracow. DFT calculations were performed using the B3LYP functional[58] together with 6-31G(d) basis set.[59] This computational level has already been successfully used in optimization and evaluation of a various organic molecules,[60-62] especially heteroatomic systems.[63-65] What is more, this computational level correlates well with experimental results.[66-68] Calculations of all critical structures were performed at temperature T = 298 K and pressure p = 1 atm in a gas phase. All localized stationary points were characterized using vibrational analysis. It was found that starting molecules as well as products had positive Hessian matrices. Analyses of global electronic properties of tested nitrones were performed according to *Domingo's* recommendations.[43,69,70] The physicochemical properties were evaluated by the SwissADME online server.[34] In order to assess a Drug-Likeness, models based on rules of *Lipinski et al.*[35] In turn, the analysis and prediction of activity spectra for the substances were prepared by the PASS online server.[36]

Acknowledgements

The presented research was supported in part by PLGrid Infrastructure. All calculations reported in this paper were performed on "Ares" supercomputer cluster in the CYFRONET center in Cracow (grant no. PLG/2023/016808).

References

1 Murahashi S. I., and Imada Y. (**2019**) Synthesis and transformations of nitrones for organic synthesis. *Chem. Rev.*, 119 (7) 4684-4716.
2 Leifert D., and Studer A. (**2023**) Organic synthesis using nitroxides. *Chem. Rev.*, 123 (16) 10302-10380.
3 Kula K., Dresler E., Demchuk O. M., and Jasiński, R. (**2015**) New aldimine N-oxides as precursors for preparation of heterocycles with potential biological activity. *Przem. Chem.*, 94 (1) 1385-1387.
4 Merino P. (**2005**) New developments in nucleophilic additions to nitrones. *C. R. Chim.*, 8 (5) 775-788.
5 Loi N., Hung P., Chinh D., and Phuong, P. (**2023**) Studying the toxicity and structure-activity relationships of some synthesized polyfunctionalized pyrimidine compounds as potential insecticides. *Curr. Chem. Lett.*, 12 (3) 489-498.
6 Abdel-Raheem S., Drar A., Hussein B., and Moustafa A. (**2023**) Some oxoimidazolidine and cyanoguanidine compounds: Toxicological efficacy and structure-activity relationships studies. *Curr. Chem. Lett.*, 12 (4) 695-704.
7 Villamena F. A., Das A., and Nash K. M. (**2012**) Potential implication of the chemical properties and bioactivity of nitrone spin traps for therapeutics. *Future Med. Chem.*, 4 (9) 1171-1207.
8 Janzen E. G. (**1971**) Spin trapping. *Acc. Chem. Res.*, 4 (1) 31-40.
9 Boyd S. L., and Boyd, R. J. (**1994**) A theoretical study of spin trapping by nitrone: trapping of hydrogen, methyl, hydroxyl, and peroxyl radicals. *J. Phys. Chem.*, 98 (45) 11705-11713.
10 Novelli G. P., Angiolini P., Tani R., Consales G., and Bordi L. (**1986**) Phenyl-t-butyl-nitrone is active against traumatic shock in rats. *Free Radical Res. Commun.*, 1 (5) 321-327.
11 Zhao Z., Cheng M., Maples K. R., Ma J. Y., and Buchan A. M. (**2001**) NXY-059, a novel free radical trapping compound, reduces cortical infarction after permanent focal cerebral ischemia in the rat. *Brain Res.*, 909 (1) 46-50.
12 Doggrell S. A. (**2006**) Nitrone spin on cerebral ischemia. *Curr. Opin. Investig. Drugs.*, 7 (1) 20-24.
13 Datta P. K., Reddy S., Sharma M., and Lianos E. A. (**2006**) Differential nephron HO-1 expression following glomerular epithelial cell injury. *Nephron. Exp. Nephrol.*, 103 (4) 131-138.
14 Mandal M. N., Moiseyev G. P., Elliott M. H., Kasus-Jacobi A., Li X., Chen H., Zheng L., Nikolaeva O., Floyd R. A., Ma J. X., and Anderson R. E. (**2011**) Alpha-phenyl-*N*-*tert*-butylnitrone (PBN) prevents light-induced degeneration of the retina by inhibiting RPE65 protein isomerohydrolase activity. *J. Biol. Chem.*, 286 (37) 32491-32501.
15 Willis C. L., and Ray D. E. (**2007**) Antioxidants attenuate MK-801-induced cortical neurotoxicity in the rat. *Neurotoxicology.* 28 (1) 161-167.
16 He T., Doblas S., Saunders D., Casteel R., Lerner M., Ritchey J. W., Snider T., Floyd R. A., and Towner, R. A. (**2011**) Effects of PBN and OKN007 in rodent glioma models assessed by 1H MR spectroscopy. *Free Radic. Biol. Med.*, 51 (2) 490-502.
17 Inoue Y., Asanuma T., Smith N., Saunders D., Oblander J., Kotake Y., Floyd R. A., and Towner, R. A. (**2007**) Modulation of Fas-FasL related apoptosis by PBN in the early phases of choline deficient diet-mediated hepatocarcinogenesis in rats. *Free Radic. Res.*, 41 (9) 972-980.

18 Zuo L., Chen Y. R., Reyes L. A., Lee H. L., Chen C. L., Villamena F. A., and Zweier, J. L. (**2009**) The radical trap 5,5-dimethyl-1-pyrroline N-oxide exerts dose-dependent protection against myocardial ischemia-reperfusion injury through preservation of mitochondrial electron transport. *J. Pharmacol. Exp. Ther.*, 329 (2) 515-523.
19 Yoshii H., Yoshii Y., Asai T., Furukawa T., Takaichi S., and Fujibayashi Y. (**2012**) Photo-excitation of carotenoids causes cytotoxicity via singlet oxygen production. *Biochem. Biophys. Res. Commun.*, 417 (1) 640-645.
20 Bosnjakovic A., and Schlick S. (**2006**) Spin trapping by 5,5-dimethylpyrroline-*N*-oxide in Fenton media in the presence of nafion perfluorinated membranes: limitations and potential. *J. Phys. Chem. B.*, 110 (22) 10720-10728.
21 Ionita P., Conte M., Gilbert B. C., and Chechik V. (**2007**) Gold nanoparticle-initiated free radical oxidations and halogen abstractions. *Org. Biomol. Chem.*, 5 (21) 3504-3509.
22 Fu H., Zhang L., Zhang S., Zhu Y., and Zhao J. (**2006**) Electron spin resonance spin-trapping detection of radical intermediates in *N*-doped TiO_2-assisted photodegradation of 4-chlorophenol. *J. Phys. Chem. B.*, 110 (7) 3061-3065.
23 Ríos-Gutiérrez M., and Domingo L. R. (**2019**) Unravelling the mysteries of the [3+2] cycloaddition reactions. *Eur. J. Org. Chem.*, 2 267-282.
24 Padwa A., and Bur S. (**2016**) Asymmetric reactions employing 1,3-dipoles. *Chem. Heterocycl. Compd.*, 52 (9) 616-626.
25 Sirotkina E. V., Efremova M. M. Starova G. L. Kuznetsov M. A., and Molchanov A. P. (**2020**) Cycloaddition of nitrones to 1,3-diarylpropenones and subsequent transformations of the resulting isoxazolidines. *Chem. Heterocycl. Compd.*, 56 (9) 1193-1201.
26 Sajadikhah S. S., and Didehban K. (**2023**) Synthesis of substituted isoxazolidines (microreview). *Chem. Heterocycl. Compd.*, 59 (9) 640-642.
27 Yıldırım A. (**2020**) Diastereoselective thermal [3+2] cycloaddition reactions of nitrone possessing an amide functional group as hydrogen bond donor/acceptor. *Chem. Heterocycl. Compd.*, 56 (3) 365-370.
28 Kula K., and Sadowski M. (**2023**) Regio-and stereoselectivity of [3+2] cycloaddition reactions between *(Z)*-1-(anthracen-9-yl)-N-methyl nitrone and analogs of trans-β-nitrostyrene on the basis of MEDT computational study. *Chem. Heterocycl. Compd.,* 59 (3) 138-144.
29 Dresler E., Wróblewska A., and Jasiński R. (**2024**) Energetic Aspects and Molecular Mechanism of 3-Nitro-substituted 2-Isoxazolines Formation via Nitrile N-Oxide [3+2] Cycloaddition: An MEDT Computational Study. *Molecules*, 29 (13) 3042.
30 Hammett L. P. (**1937**) The effect of structure upon the reactions of organic compounds. Benzene derivatives. *J. Am. Chem. Soc.*, 59 (1) 96-103.
31 Taft R. W. (**1960**) Sigma values from Reactivities[1]. *J. Phys. Chem.*, 64 (12) 1805-1815.
32 Brown H. C., and Okamoto Y. (**1958**) Electrophilic substituent constants. *J. Am. Chem. Soc.*, 80 (18) 4979-4987.
33 Exner O. (**1966**) Studies on the inductive effect. V. Separation of inductive and mesomeric effects in meta and para benzene derivatives. *Collect. Czech. Chem. Commun.*, 31 (1) 65-89.
34 SwissADME. Available online: http://www.swissadme.ch/ (accessed on 12 July 2024).
35 Lipinski C.A., Lombardo F., Dominy B. W., and Feeney P. J. (**2001**) Experimental and computational approaches to estimate solubility and permeability in drug discovery and development settings. *Adv. Drug Deliv. Rev.*, 46 (1) 3-26.
36 PASS Online. Available online: http://www.way2drug.com/passonline/ (accessed on 12 July 2024).
37 Soldaini G., Cardona F., and Goti A. (**2007**) Catalytic oxidation of imines based on methyltrioxorhenium/urea hydrogen peroxide: A mild and easy chemo-and regioselective entry to nitrones. *Org. Lett.*, 9 (3) 473-476.
38 Tang C., Shao J., Si C., Yang X., Hu X., Li P., and Wang X. (**2024**) Discovery of indole-3-acetic acid derivatives containing 1,3,4-thiadiazole thioether and amide moieties as novel antibacterial agents. *Chem. Heterocycl. Compd.*, 60 (1/2) 92-98.
39 Mitsui H., Zenki S. I., Shiota T., and Murahashi S. I. (**1984**) Tungstate catalysed oxidation of secondary amines with hydrogen peroxide. A novel transformation of secondary amines into nitrones. *J. Chem. Soc. Chem. Commun.*, 13 874-875.
40 Izmest'ev A. N., Isakov S. S., Kravchenko A. N., and Gazieva G. A. (**2024**) The synthesis and antitumor activity of novel 1-alkyl-3-phenyland 3-alkyl-1-phenylimidazothiazolotriazines. *Chem. Heterocycl. Compd.*, 60 (3/4) 133-137.
41 Mohammed J. H., and Salih N. A. M. (**2022**) Synthesis and characterization of some new nitrones derivatives and screening their biological activities. *J. Zhejiang Univ. Sci.*, 10 (4) 268-273.
42 Gomonov K. A., Pelipko V. V., Litvinov I. A., Baichurin R. I., and Makarenko S. V. (**2024**) Synthesis and structure of new substituted furan-3-carboxylate hydrazones. *Chem. Heterocycl. Compd.*, 60 (3/4) 196-204.
43 Tikhomolova A. S., Mamleeva Z. V., and Egorova A. Y. (**2024**) An efficient synthesis of (E)-3-[(dimethylamino) methylidene] furan-2 (3H)-thiones and transamination reactions thereof. *Chem. Heterocycl. Compd.*, 60 (3) 138-142.
44 Domingo L. R., Ríos-Gutiérrez M., and Pérez P. (**2016**) Applications of the Conceptual Density Functional Theory Indices to Organic Chemistry Reactivity. *Molecules*, 21 (6) 748.
45 Ameur S., Barhoumi A., Ríos-Gutiérrez M., Aitouna A. O., Abdallaoui H. E. A. E., Mazoir N., Belghiti M. E., Syed A., Zeroual A., and Domingo L. R. (**2023**) A MEDT study of the mechanism and selectivity of the hetero-Diels–Alder reaction between 3-benzoylpyrrolo[1,2-c][1,4]-benzoxazine-1,2,4-trione and vinyl acetate. *Chem. Heterocycl. Compd.*, 59 (3) 165-170.
46 Raji H., Aitouna A. O., Barhoumi A., Hammal R., Chekroun A., Zeroual A., Benharref A. and Mazoir, N. (**2023**) [2+1] Cycloaddition reaction of α-atlantone with m-CPBA in the light of experimental and MEDT quantum-chemical study. *Chem. Heterocycl. Compd.*, 59 (3) 112-117.
47 Messaadia S., Nacereddine A. K., and Djerourou A. (**2023**) Exploring the factors controlling the mechanism and the high stereoselectivity of the polar [3+ 2] cycloaddition reaction of the N, N'-cyclic azomethine imine with 3-nitro-2-phenyl-2 H-chromene. A molecular electron density theory study. *Chem. Heterocycl. Compd.*, 59 (3) 128-137.
48 Abdoul-Hakim M., Idrissi K. E., Zeroual A., and Garmes H. (**2023**) Investigation of the solvent effect, regioselectivity, and the mechanism of the cycloaddition reaction between 2-chlorobenzimidazole and benzonitrile oxide. *Chem. Heterocycl. Compd.*, 59 (3) 155-164.
49 Jaffe H. H. (**1953**) A reexamination of the Hammett equation. *Chem. Rev.*, 53 (2) 191-261.
50 Pavlinac I. B., Starčević K., Persoons L., Banjanac M., Radovanović V., Daelemans D., and Hranjec M. (**2024**) Novel

iminocoumarin imidazo[4,5-b]pyridine derivatives: design, synthesis, and biological evaluation. *Chem. Heterocycl. Compd.*, 60 (1/2) 205-208.
51 Sharapov A. D., Fatykhov R. F., and Khalymbadzha I. A. (**2024**) Synthesis of fluorophores based on benzo[g]coumarin framework (microreview). *Chem. Heterocycl. Compd.*, 60 (1/2) 26-28.
52 Acharjee N., Banerji A., Banerjee M., and Das T. K. (**2009**) 1,3-Dipolar cycloadditions. Part XVII: Experimental and theoretical spectroscopic investigations of C-aryl-N-methyl nitrones. *Indian J. Chem.*, 48 (12) 1627-1637.
53 Tyrrell E., Allen J., Jones K., and Beauchet R. (**2005**) Asymmetric 1,3-dipolar cycloaddition reactions of nitrones with (S)-(-)-4-benzyl-N-methacryloyl-2-oxazolidinone. *Synthesis*, 14 2393-2399.
54 Vorontsova S. K., Scherbakov A. M., Minyaev M. E., Menchikov L. G., and Zavarzin I. V. (**2024**) The synthesis of furazano- and thiadiazolopyrazine steroids and their antiproliferative activity. *Chem. Heterocycl. Compd.*, 60 (3/4) 205-208.
55 Komkov A. V., Menchikov L. G., Dmitrenok A. S., Kolotyrkina N. G., and Zavarzin I. V. (**2024**) A method for the synthesis of spiro-1, 3, 4-thiadiazolines. *Chem. Heterocycl. Compd.*, 60 (3/4) 183-189.
56 Dubina T. F., Kosarevych A. V., Kucher O. V., Sosunovych B. S., Smolii O. B., Vashchenko B. V., and Grygorenko O. O. (**2024**) Synthesis and reactions of novel imidazo [4, 5-b] pyridine building blocks. *Chem. Heterocycl. Compd.*, 60 (3/4) 175-182.
57 Frisch M. J., Trucks G. W., Schlegel H. B., Scuseria G. E., Robb M. A., Cheeseman J. R., Montgomery J. A., Vreven T. J., Kudin K. N., Burant J. C., Millam J. M., Iyengar S. S., Tomasi J., Barone V., Mennucci B., Cossi M., Scalmani G., Rega N., Petersson G. A., Nakatsuji H., Hada M., Ehara M., Toyota K., Fukuda R., Hasegawa J., Ishida M., Nakajima Y., Honda O., Kitao O., Nakai H., Klene M., Li X., Knox J. E., Hratchian H. P., Cross J. B., Adamo C., Jaramillo J., Gomperts R., Stratmann R. E., Yazyev O., Austin A. J., Cammi R., Pomelli C., Ochterski J. W., Ayala P. Y., Morokuma K., Voth G. A., Salvador P., Dannenberg J. J., Zakrzewski V. G., Dapprich S., Daniels A. D., Strain M. C., Farkas M. C., Malick D. K., Rabuck A. D., Raghavachari K., Foresman J. B., Ortiz J. V., Cui Q., Baboul A. G., Clifford S., Cioslowski J., Stefanov B. B., Liu G., Liashenko A., Piskorz P., Komaromi I., Martin R. L., Fox D. J., Keith T., Al-Laham M. A., Peng C. Y., Nanayakkara A., Challacombe M., Gill P. M. W., Johnson B., Chen W., Wong M. W., Gonzalez C., and Pople J. A. (**2009**) Gaussian 09 rev A.1 Gaussian Inc. Wallingford CT, USA.
58 Tirado-Rives J., and Jorgensen W. L. (**2008**) Performance of B3LYP density functional methods for a large set of organic molecules. *J. Chem. Theory Comput.*, 4 (2) 297-306.
59 Petersson A., Bennett A., Tensfeldt T. G., Al-Laham M. A., Shirley W. A., and Mantzaris J. (**1988**) A complete basis set model chemistry. I. The total energies of closed-shell atoms and hydrides of the first-row elements. *J. Chem. Phys.*, 89 (4) 2193-2218.
60 Mondal A., and Acharjee N. (**2023**) Unveiling the exclusive stereo and site selectivity in [3+2] cycloaddition reactions of a tricyclic strained alkene with nitrile oxides from the molecular electron density theory perspective. *Chem. Heterocycl. Compd.*, 59 (3) 145-154.
61 Yousfi Y., Benchouk W. and Mekelleche S. M. (**2023**) Prediction of the regioselectivity of the ruthenium-catalyzed [3+2] cycloadditions of benzyl azide with internal alkynes using conceptual DFT indices of reactivity. *Chem. Heterocycl. Compd.*, 59 (3) 118-127.
62 Woliński P., Kącka-Zych A., Dziuk B., Ejsmont K., Łapczuk-Krygier A., and Dresler E. (**2019**) The structural aspects of the transformation of 3-nitroisoxazoline-2-oxide to 1-aza-2,8-dioxabicyclo[3.3.0]octane derivatives: Experimental and MEDT theoretical study. *J. Mol. Struct.*, 1192 27-34;
63 Siadati S. A., Kula K., and Babanezhad E. (**2019**) The possibility of a two-step oxidation of the surface of C20 fullerene by a single molecule of nitric (V) acid. *Chem. Rev. Lett.*, 2 (1) 2-6.
64 Zawadzińska K., and Kula K. (**2021**) Application of β-phosphorylated nitroethenes in [3+2] cycloaddition reactions involving benzonitrile N-oxide in the light of DFT computational study. *Organics*, 2 (1) 26-37.
65 Łapczuk-Krygier A., Jaśkowska J., and Jasiński R. (**2018**) The influence of Lewis acid catalyst on the kinetic and molecular mechanism of nitrous acid elimination from 5-nitro-3-phenyl-4,5-dihydroisoxazole: DFT computational study. *Chem. Heterocycl. Comp.*, 54 1172-1174.
66 Chafaa F., and Nacereddine A. K. (**2023**) A molecular electron density theory study of mechanism and selectivity of the intramolecular [3+2] cycloaddition reaction of a nitrone–vinylphosphonate adduct. *Chem. Heterocycl. Compd.*, 59 (3) 171-178.
67 Domingo L. R., Kula K., Rios-Gutierrez M., and Jasinski R. (**2021**) Understanding the Participation of Fluorinated Azomethine Ylides in Carbenoid-Type [3+ 2] Cycloaddition Reactions with Ynal Systems: A Molecular Electron Density Theory Study. *J. Org. Chem.*, 86 (18) 12644-12653.
68 Domingo L. R., Kula K., and Ríos-Gutiérrez M. (**2020**) Unveiling the reactivity of cyclic azomethine ylides in [3+2] cycloaddition reactions within the molecular electron density theory. *Eur. J. Org. Chem.*, 37 5938-5948.
69 Parr R. G., Szentpály L., and Liu S. (**1999**) Electrophilicity index. *J. Am. Chem. Soc.*, 121 (9) 1922-1924.
70 Parr R.G., Gadre S. R., and Bartolotti L. J. (**1979**) Local density functional theory of atoms and molecules. *Proc. Natl. Acad. Sci.*, 76 (6) 2522-2526.